Amide Formation from Aldimine and Water Promoted by Coordinated Metal Redox. Chemistry of a Family of Isomeric $Ru^{II}(diimine)_2Cl_2$, $Ru^{III}(diimine)_2Cl_2^+$, and $Ru^{III}(diimine)(amide-imine)Cl_2$ Complexes

Mahua Menon, Amitava Pramanik, and Animesh Chakravorty*

Department of Inorganic Chemistry, Indian Association for the Cultivation of Science, Calcutta 700 032, India

Received December 16, 1994[⊗]

The relevant N,N-coordinating ligands are RN=C(H)−C(H)=NR (general abbreviation D, specific abbreviations D^1 and D^2 for R = cyclohexyl and *p*-tolyl, respectively) and [RN=C(H)−C(=O)−NR]$^-$ (abbreviations A, A^1, A^2). Oxidation of *cis*- and *trans*-$Ru^{II}D_2Cl_2$ by aqueous cerium(IV) (H_2O_2 can also be used for *trans*-RuD_2Cl_2) affords in excellent yield the amide complexes *cis*- and *trans*-$Ru^{III}DACl_2$ with retention of parental isomeric structure. Spectral and magnetic characterization data of the complexes are reported along with the X-ray structures of *cis*-$RuD^1{}_2Cl_2$·PhMe and *cis*-$RuD^1A^1Cl_2$·CH_2Cl_2. The ruthenium(III)−ruthenium(II) couples of the complexes follow $E_{1/2}$ systematics (other things remaining the same in each case): geometry, cis > trans; ligand, D > A; substituent, *p*-tolyl > cyclohexyl. The $Ru^{III}D_2Cl_2^+$ moiety has been electrogenerated in solution, and *cis*-$[Ru^{III}D^1{}_2Cl_2]ClO_4$ has been isolated and characterized in the pure state. The conversion $RuD_2Cl_2 \rightarrow RuDACl_2$ actually occurs via $RuD_2Cl_2^+$, which reacts with water, affording the amide complex. The reaction is first order with respect to both $RuD_2Cl_2^+$ and H_2O, and the activation parameters are $\Delta H^{\ddagger} = 12.5$ kcal mol^{-1} and $\Delta S^{\ddagger} = -29.8$ eu in the case of *trans*-$RuD^2{}_2Cl_2$. It is proposed that the water molecule adds to the azomethine function and the α-hydroxy amine function of the adduct is rapidly oxidized via an induced electron transfer pathway. The net reactions are as follows: $RuD_2Cl_2 \rightarrow RuD_2Cl_2^+ + e$; $RuD_2Cl_2^+ + H_2O \rightarrow RuDACl_2 + 2e + 3H^+$. A crucial reaction condition appears to be the easy accessibility of two oxidation states of the metal ion related by facile transfer of one electron, the higher oxidation state being sufficiently polarizing to induce water binding at the aldimine site. Crystal data for the complexes are as follows: *cis*-$RuD^1{}_2Cl_2$·PhME, crystal system monoclinic, space group $P2_1/c$, $a = 14.808(6)$ Å, $b = 19.442(7)$ Å, $c = 13.989(6)$ Å, $\beta = 117.18(3)°$, $V = 3583(2)$ Å^3, $Z = 4$, $R = 3.70\%$, $R_w = 4.31\%$; *cis*-$RuD^1A^1Cl_2$·CH_2Cl_2, crystal system monoclinic, space group $P2_1/c$, $a = 11.295(4)$ Å, $b = 27.064(14)$ Å, $c = 12.064(4)$ Å, $\beta = 107.52(2)°$, $V = 3517(2)$ Å^3, $Z = 4$, $R = 6.53\%$, $R_w = 6.95\%$.

Introduction

Incorporation of oxygen functions into organic substrates assisted by metal coordination is a reaction class of fundamental import in chemistry. This work is concerned with the reaction of eq 1 where the functional transformation aldimine → amide

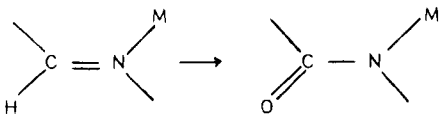

(1)

occurs. Our objectives are to search for reactive systems and to scrutinize the scope and nature of this interesting but little-known reaction. Recently we observed that certain pyridine-2-carboxaldimine complexes of rhenium and ruthenium incorporating the chelate motif **1** undergo the transformation of eq 1.[1,2] This has prompted us to explore chelates of simple α-diimines as possible reactive substrates. We were encouraged by the reports that amides are among the products of the otherwise complicated oxidation of α-diimine chelates of iron.[3]

Herein we disclose the facile and clean conversion of the ruthenium α-diimine motif **2** to the amide−imine motif **3**. A

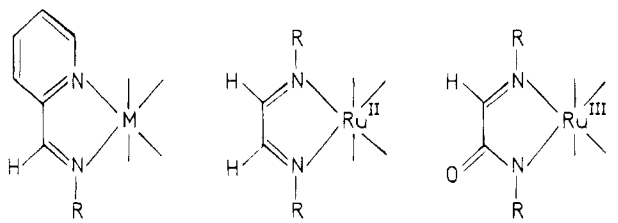

1 **2** **3**

family of parent and product complexes have been characterized. Isomeric metal geometries are conserved in the reaction which proceeds via metal oxidation and ligand aquation and oxidation. Certain general governing principles are defined.

Results and Discussion

Parent α-Diimine Complexes. These are of the known[4,5] general types *cis*- and *trans*-$Ru^{II}D_2Cl_2$, **4a** and **4b** (D = α-diimine, Figure 1). The two R groups used here are cyclohexyl (D = D^1) and *p*-tolyl (D = D^2). Our preparative methods are summarized in Scheme 1. We have found Ru(Me$_2$-

* Telefax: +91-33-473-2805. Email: icac@iacs.ernet.in.

⊗ Abstract published in *Advance ACS Abstracts,* May 15, 1995.

(1) Menon, M.; Pramanik, A.; Bag, N.; Chakravorty, A. *Inorg. Chem.* **1994**, *33*, 403.
(2) Menon, M.; Choudhury, S.; Pramanik, A.; Deb, A. K.; Chandra, S. K.; Bag, N.; Goswami, S.; Chakravorty, A. *J. Chem. Soc., Chem. Commun.* **1994**, 57.
(3) (a) Chum, H. L.; Krumholtz, P. *Inorg. Chem.* **1974**, *13*, 514. (b) Chum, H. L.; Krumholtz, P. *Inorg. Chem.* **1974**, *13*, 519. (c) Chum, H. L.; Rabockai, T.; Phillips, J.; Osteryoung, R. A. *Inorg. Chem.* **1977**, *16*, 812. (d) Chum, H. L.; Helene, M. E. M. *Inorg. Chem.* **1980**, *19*, 876.
(4) tom Dieck, H.; Kollvitz, W.; Kleinwachter, I. *Inorg. Chem.* **1984**, *23*, 2685.
(5) Pank, V.; Klaus, J.; von Deuten, K.; Fiegel, M.; Bruder, H.; tom Dieck, H. *Transition Met. Chem.* **1981**, *6*, 185.

0020-1669/95/1334-3310$09.00/0

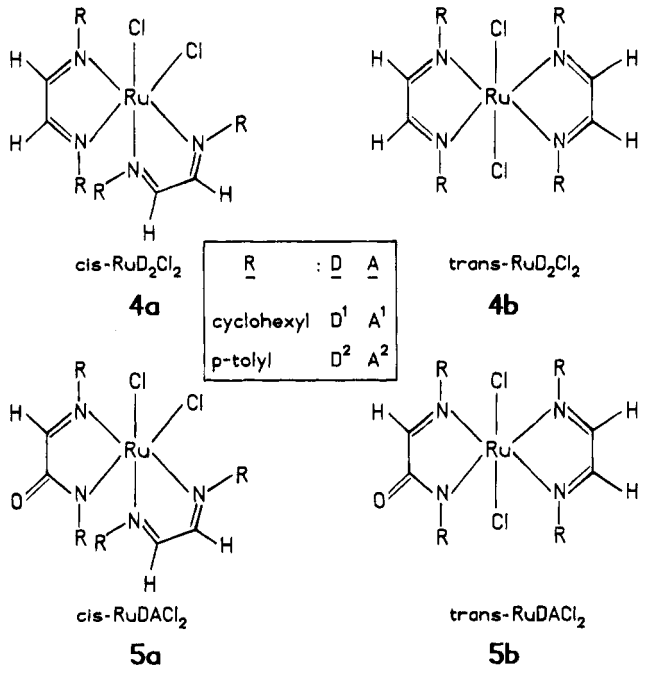

Figure 1. Parent (**4a**, **4b**) and product (**5a**, **5b**) complexes.

Scheme 1[a]

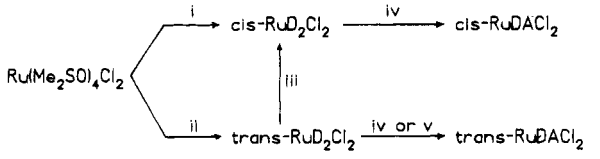

[a]Conditions : (i) D = D^1 : EtOH, reflux; (ii) D = D^1 : EtOH, warm 40°C; D = D^2 : EtOH, reflux; (iii) D = D^1 : EtOH, reflux; D = D^2 : diglyme, reflux; (iv) D = D^1, D^2 : CH_2Cl_2-CH_3CN (1:6), $(NH_4)_4[Ce(SO_4)_4].2H_2O$-$H_2O$, stir; (v) D = D^1, D^2 : CH_2Cl_2-CH_3CN (1:6), 30% H_2O_2, stir.

$SO)_4Cl_2$ to be an excellent and generally applicable starting material for synthesis. All four complexes have been isolated in stable forms. Earlier, *trans*-$RuD^1{}_2Cl_2$ was observed only as an occasional product in a different synthetic method.[4]

Amide Complexes. Synthesis. Oxidation of *cis*- and *trans*-RuD_2Cl_2 with aqueous cerium(IV) afford, in excellent yields, the dark-colored amide complexes of trivalent ruthenium *cis*- and *trans*-$Ru^{III}DACl_2$, **5a** and **5b** (Figure 1), with retention of parental isomeric structure (Scheme 1). While D is neutral, the amide−imine ligand is N-bonded to ruthenium(III) in the anionic deprotonated form, A^-. Specific A's are A^1 (R = cyclohexyl) and A^2 (R = *p*-tolyl). Even when excess oxidant is used, only one imine function in one of the α-diimine ligands is oxidized to amide; the second diimine ligand remains unaffected. Thus $RuDACl_2$ is the only product of oxidation.

Spectra. Selected spectral data are set out in Tables 1 and 2. The paramagnetic (t_2^5, $S = {}^1/_2$, Table 2) $RuDACl_2$ complexes exhibit amide bands in the IR region (1590−1630 cm^{-1}), LMCT excitation in the visible region (Table 1), a relatively weak feature in the near-IR region (1400−1800 nm, Table 1, Figure 2), and rhombic EPR spectra (Table 2, Figure 2).

The EPR spectra have been analyzed[6] with the help of d^5 *g*-tensor theory.[7,8] We only quote here the important result that in each case the computed energy of a ligand field transition within the t_2 shell split by low-symmetry components fits well with the energy of the observed near-IR band (Table 2). For

(6) Menon, M.; Pramanik, A.; Chakravorty, A. Unpublished results.

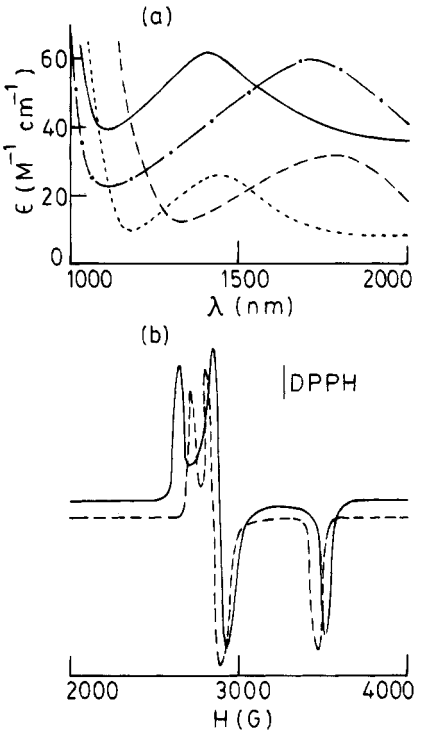

Figure 2. (a) Near-IR spectra of *cis*-$RuD^2{}_2Cl_2^+$ (— —), *trans*-$RuD^2{}_2Cl_2^+$ (- - -), *cis*-$RuD^2A^2Cl_2$ (— • —), and *trans*-$RuD^2A^2Cl_2$ (—) in dichloromethane solution. (b) X-Band EPR spectra of *cis*-$RuD^2{}_2Cl_2^+$ (— — —) and *trans*-$RuD^2A^2Cl_2$ (—) in dichloromethane−toluene glass at 77 K.

isomeric $RuDACl_2$ complexes, both the predicted and observed energies of the band follow the order trans > cis. This trend is also consistent with ligand field description of t_2 splitting.[9] The trans > cis inequality is of diagnostic value for isomeric structure assignment.

The optical spectra of the RuD_2L_2 isomers have a dominant MLCT band in this visible region (Table 1) in general agreement with previous findings.[4]

Structure. The imine → amide oxidation process has been authenticated by structure determination in the one case where single crystals could be successfully grown (as solvates): *cis*-$RuD^1{}_2Cl_2$·PhMe and *cis*-$RuD^1A^1Cl_2$·CH_2Cl_2. Molecular views of the two complexes excluding solvents of crystallization are shown in Figures 3 and 4. Selected bond distances and angles are listed in Tables 3 and 4.

Both complexes have the *cis*-RuN_4Cl_2 configuration showing that the oxidation process is stereoretentive. The cyclohexyl groups in the complexes uniformly have chair conformation. The amide function in the oxidized complex lies trans to a chlorine site. In this manner the three anionic donors (amide N, two chlorides) are positioned meridionally. The possible facial isomer which would have formed if oxidation occurred cis to a chlorine site has not been observed in any of the oxidations.

(7) (a) Bleaney, B.; O'Brien, M. C. M. *Proc. Phys. Soc. London, Sect. B* **1956**, *69*, 1216. (b) Griffith, J. S. *The Theory of Transition Metals Ions*; Cambridge University Press: Cambridge, 1961; p 364.

(8) (a) Lahiri, G. K.; Bhattacharya, S.; Ghosh, B. K.; Chakravorty, A. *Inorg. Chem.* **1987**, *26*, 4324. (b) Lahiri, G. K.; Bhattacharya, S.; Mukherjee, M.; Mukherjee, A. K.; Chakravorty, A. *Inorg. Chem.* **1987**, *26*, 3359.

(9) (a) Yamatera, H. *Bull. Chem. Soc. Jpn.* **1958**, *31*, 95. (b) McClure, D. S. *Advances in Chemistry of Coordination Compounds*; The Macmillan Co.: New York, 1961; p 498. (c) Schaffer, C. E. *Struct. Bonding* **1973**, *14*, 69. (d) Lever, A. B. P. *Inorganic Electronic Spectroscopy*, 2nd ed.; Elsevier: Amsterdam 1984; p 52.

Table 1. Electronic Spectral[a] and IR[b] Data at 298 K

compound	UV–vis–near-IR data λ_{max}, nm (ϵ, M^{-1} cm^{-1})	IR data ν, cm^{-1}
cis-$RuD^1{}_2Cl_2$	715[c] (490), 530 (8960), 475[c] (2990)	1630
trans-$RuD^1{}_2Cl_2$	1185[c] (260), 1075[c] (280), 655 (7035), 515[c] (3370), 450[c] (1560)	1620
cis-$RuD^2{}_2Cl_2$	825[c] (120), 575 (8400), 475[c] (2580), 370 (13 630)	1600
trans-$RuD^2{}_2Cl_2$	810[c] (2480), 700 (9590), 555[c] (1560), 425 (11 600)	1600
cis-$RuD^1A^1Cl_2$	1800 (79), 525 (4230), 432[c] (2980), 382 (3770)	1593, 1620
trans-$RuD^1A^1Cl_2$	1475 (64), 585 (3810), 385 (3760)	1590, 1620
cis-$RuD^2A^2Cl_2$	1730 (60), 580[c] (3000), 535[c] (3000), 390 (12 823)	1600, 1630
trans-$RuD^2A^2Cl_2$	1400 (62), 615 (3370), 505 (3340), 385 (9210)	1605, 1625
cis-$RuD^1{}_2Cl_2^+$	1825 (42), 600[c] (1250), 500[c] (2870), 415 (3040)	
trans-$RuD^1{}_2Cl_2^+$	1475 (72), 630[c] (760), 530 (2560), 430 (3540)	
cis-$RuD^2{}_2Cl_2^+$	1800 (32), 730[c] (1000), 540[c] (6350), 382 (21 043)	
trans-$RuD^2{}_2Cl_2^+$	1435 (26), 675[c] (1100), 550[c] (4400), 445 (15 160)	

[a] The solvent is dichloromethane. [b] In KBr disk. [c] Shoulder.

Table 2. Bulk Magnetic Moments,[a] EPR g Values,[b] and Near-IR Transitions

compound	μ_{eff}, μ_B	g_1	g_2	g_3	ν_{calc}, cm^{-1}	ν_{obsd}, cm^{-1}
cis-$RuD^1A^1Cl_2$	1.92	2.344	2.283	1.886	6187	5560
trans-$RuD^1A^1Cl_2$	1.90	2.456	2.297	1.865	6373	6780
cis-$RuD^2A^2Cl_2$	1.89	2.478	2.289	1.905	5155	5780
trans-$RuD^2A^2Cl_2$	1.87	2.476	2.279	1.870	6828	7140
cis-$RuD^1{}_2Cl_2^+$	1.90[c]	2.488	2.331	1.847	5954	5480
trans-$RuD^1{}_2Cl_2^+$		2.601	2.321	1.821	6211	6780
cis-$RuD^2{}_2Cl_2^+$		2.424	2.313	1.900	5286	5560
trans-$RuD^2{}_2Cl_2^+$		2.578	2.315	1.843	6612	6970

[a] In solid state at 298 K. [b] In 1:1 dichloromethane–toluene frozen glass (77 K). [c] Value given for the isolated perchlorate salt.

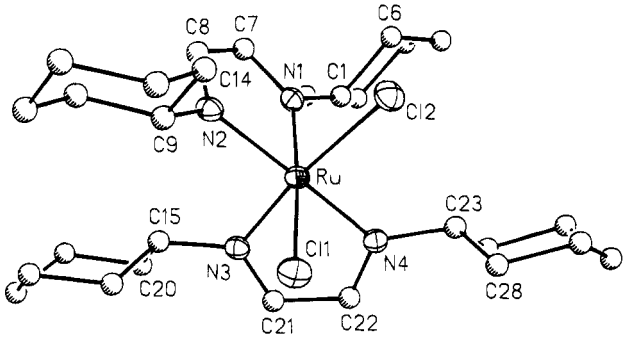

Figure 3. Perspective view (probability ellipsoids at 40% level) and atom-labeling scheme for *cis*-$RuD^1{}_2Cl_2$·PhMe.

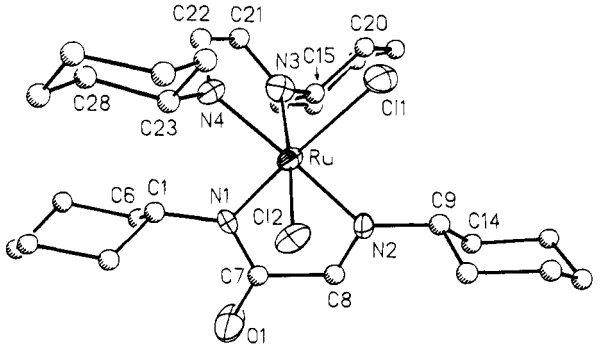

Figure 4. Perspective view (probability ellipsoids at 40% level) and atom-labeling scheme for *cis*-$RuD^1A^1Cl_2$·CH_2Cl_2.

The average Ru–N length in the RuD^1 chelate ring is *longer* by ~0.02 Å in $RuD^1A^1Cl_2$ compared to that in $RuD^1{}_2Cl_2$. This can be attributed to the inferior back-bonding ($t_2(Ru) \rightarrow \pi^*(D)$) ability of ruthenium(III) compared to ruthenium(II).[10] The average lengths of the Ru–Cl bond (no back-bonding) expectedly shows the reverse trend, being *shorter* in the amide complex by 0.04 Å.

Table 3. Selected Bond Distances (Å) and Angles (deg) and Their Estimated Standard Deviations for *cis*-$RuD^1{}_2Cl_2$·PhMe

Ru–Cl(1)	2.422(3)	N(1)–C(7)	1.303(8)
Ru–Cl(2)	2.428(2)	N(2)–C(8)	1.292(10)
Ru–N(1)	2.008(6)	N(4)–C(22)	1.303(7)
Ru–N(2)	2.055(5)	N(3)–C(21)	1.287(8)
Ru–N(3)	2.010(4)	C(7)–C(8)	1.429(9)
Ru–N(4)	2.031(4)	C(21)–C(22)	1.419(7)
Cl(1)–Ru–Cl(2)	91.1(1)	Cl(1)–Ru–N(1)	174.2(1)
Cl(2)–Ru–N(1)	88.1(1)	Cl(1)–Ru–N(2)	96.3(2)
Cl(2)–Ru–N(2)	88.9(1)	N(1)–Ru–N(2)	78.0(2)
Cl(1)–Ru–N(3)	87.3(2)	Cl(2)–Ru–N(3)	172.6(1)
N(1)–Ru–N(3)	94.2(2)	N(2)–Ru–N(3)	98.5(2)
Cl(1)–Ru–N(4)	86.9(2)	Cl(2)–Ru–N(4)	94.8(1)
N(1)–Ru–N(4)	98.8(2)	N(2)–Ru–N(4)	175.1(2)
N(3)–Ru–N(4)	77.9(2)		

Table 4. Selected Bond Distances (Å) and Angles (deg) and Their Estimated Standard Deviations for *cis*-$RuD^1A^1Cl_2$·CH_2Cl_2

Ru–Cl(1)	2.376(4)	N(1)–C(7)	1.356(15)
Ru–Cl(2)	2.377(5)	N(2)–C(8)	1.255(16)
Ru–N(1)	1.986(9)	N(4)–C(22)	1.265(22)
Ru–N(2)	2.083(9)	N(3)–C(21)	1.281(14)
Ru–N(3)	2.049(12)	C(7)–C(8)	1.491(17)
Ru–N(4)	2.049(9)	C(21)–C(22)	1.423(25)
C(7)–O(1)	1.220(17)		
Cl(1)–Ru–Cl(2)	93.9(2)	Cl(1)–Ru–N(1)	170.4(3)
Cl(2)–Ru–N(1)	92.6(4)	Cl(1)–Ru–N(2)	93.3(3)
Cl(2)–Ru–N(2)	85.4(3)	N(1)–Ru–N(2)	80.1(3)
Cl(1)–Ru–N(3)	84.4(3)	Cl(2)–Ru–N(3)	172.5(3)
N(1)–Ru–N(3)	90.0(4)	N(2)–Ru–N(3)	102.0(4)
Cl(1)–Ru–N(4)	89.2(3)	Cl(2)–Ru–N(4)	94.7(4)
N(1)–Ru–N(4)	97.3(3)	N(2)–Ru–N(4)	177.5(3)
N(3)–Ru–N(4)	78.0(4)		

The coordinated amide function in $RuD^1A^1Cl_2$ deviates significantly from planarity, corresponding to a rotation around the N(1)-C(7) bond by 10.8°, which is also the dihedral angle between the nearly perfect planes of Ru, N(1), C(1), and C(7) (mean deviation 0.004 Å) and of N(1), C(7), O(1), and C(8) (mean deviation 0.012 Å) in the RuA^1 chelate ring. The Ru–N(1), N(1)–C(7), and C(7)–O(1) lengths in our complex compare well with the corresponding lengths of the coordinated amide function in $Ru^{III}(NH_3)_4$(glycinamidato)$^{2+}$.[11]

Although single crystals could not be grown for the other complexes concerning us here, the present structural results taken collectively with spectroscopic data considered above and

(10) (a) Richardson, D. E.; Walker, D. D.; Sutton, J. E.; Hodgson, K. O.; Taube, H. *Inorg. Chem.* **1979**, *18*, 2216. (b) Wishart, J. F.; Bino, A.; Taube, H. *Inorg. Chem.* **1986**, *25*, 3318. (c) Gress, M. E.; Creutz, C.; Quicksall, C. O. *Inorg. Chem.* **1981**, *20*, 1522. (d) Eggleston, D. S.; Goldsby, K. A.; Hodgson, D. J.; Meyer, T. J. *Inorg. Chem.* **1985**, *24*, 4573.

(11) Ilan, Y.; Kapon, M. *Inorg. Chem.* **1986**, *25*, 2350.

Table 5. Cyclic Voltammetric Formal Potentials of Isomers in Dichloromethane (0.1 M TEAP) at a Platinum Electrode at 298 K[a-d]

compound	Ru^{III}/Ru^{II} $E_{1/2}$, V (ΔE_p, mV)	compound	Ru^{III}/Ru^{II} $E_{1/2}$, V (ΔE_p, mV)
cis-$RuD^1{}_2Cl_2$	0.55 (60)	*cis*-$RuD^1A^1Cl_2$	−0.16 (80)
trans-$RuD^1{}_2Cl_2$	0.25 (60)	*trans*-$RuD^1A^1Cl_2$	−0.30 (80)
cis-$RuD^2{}_2Cl_2$	0.60 (80)	*cis*-$RuD^2A^2Cl_2$	0.01 (80)
trans-$RuD^2{}_2Cl_2$	0.44 (80)	*trans*-$RuD^2A^2Cl_2$	−0.08 (80)

[a] Scan rate 50 mV s^{-1}. [b] $E_{1/2} = {}^1/_2(E_{pa} + E_{pc})$ where E_{pa} and E_{pc} are the anodic and cathodic peak potentials, respectively. [c] $\Delta E_p = E_{pa} - E_{pc}$. [d] Reference electrode, SCE.

electrochemical findings noted below testify to the correctness of the geometrical structures of the complexes as presented in Figure 1. Last, we note that the bond parameters of *cis*-$RuD^1{}_2Cl_2$ are similar to those of **4a** (R = isopropyl).[5]

Metal Redox. Both RuD_2Cl_2 and $RuDACl_2$ display nearly reversible (peak-to-peak separation, 60−80 mV) one-electron cyclic voltammetric responses due to stereoretentive ruthenium(III)−ruthenium(II) redox, eqs 2 and 3. The crucially important $RuD_2Cl_2^+$ species will be considered further in the next section.

$$cis/trans\text{-}Ru^{III}D_2Cl_2^+ + e \rightleftharpoons cis/trans\text{-}Ru^{II}D_2Cl_2 \quad (2)$$

$$cis/trans\text{-}Ru^{III}DACl_2 + e \rightleftharpoons cis/trans\text{-}Ru^{II}DACl_2^- \quad (3)$$

Certain trends of the reduction potentials ($E_{1/2}$ vs SCE) listed in Table 5 will now be noted. For low-spin $t_2^5-t_2^6$ couples, the trend cis > trans which is observed in the present complexes is diagnostic of isomeric structures.[12,13] This arises from the better stabilization of the t_2^6 (ruthenium(II)) configuration in the cis compared to the trans configuration via back-bonding.

For a given R and geometry, the $E_{1/2}$ of $RuDACl_2$ is lower than that of RuD_2Cl_2 by a remarkable 0.5−0.6 V. The better stabilization of the ruthenium(III) state by the deprotonated amide function (A^-) compared to aldimine function is also reflected in bond lengths of $RuD^1A^1Cl_2$: the Ru−N(amide) length is shorter than the average Ru−N(imine) lengths by 0.07 Å (Table 4). Last, we note that the $E_{1/2}$ of any R = *p*-tolyl complex is higher than that of the *R* = cyclohexyl congener because the cyclohexyl group is a better electron donor than the *p*-tolyl group.

$Ru^{III}D_2Cl_2^+$. This species is the oxidant in the ruthenium(III)−ruthenium(II) couple of eq 2. It is shown in the next section that the conversion of RuD_2Cl_2 to $RuDACl_2$ proceeds via $RuD_2Cl_2^+$. Characterization data for the latter are given here.

The $RuD_2Cl_2^+$ cation has been quantitatively generated in dry dichloromethane solution by coulometric oxidation of RuD_2Cl_2. In the case of *cis*-$RuD^1{}_2Cl_2^+$, the complex has been isolated in the pure state as the perchlorate salt (μ_{eff} = 1.90 μ_B; Λ = 132 Ω^{-1} cm^2 M^{-1} in acetonitrile solution). The electronic and EPR spectra of the complexes are given in Figure 2 and the data are given in Tables 1 and 2. As in the case of $RuDACl_2$,

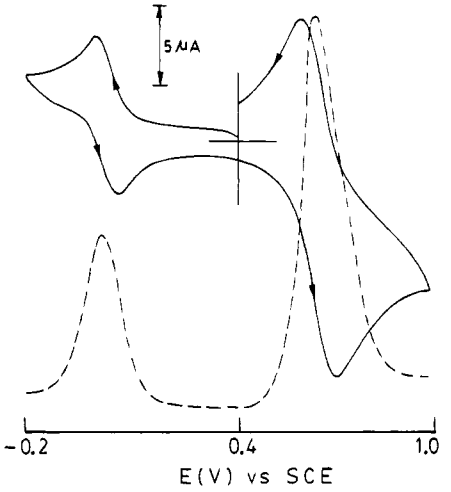

Figure 5. Cyclic (—) and differential pulse (− − −) voltammograms of the product resulting from the completed reaction of *cis*-$RuD^2{}_2Cl_2^+$ with water in MeCN solution. The two responses (current heights 2:1) correspond to the couples *cis*-$RuD^2{}_2Cl_2^+$−*cis*-$RuD^2{}_2Cl_2$ (higher potential) and *cis*-$RuD^2A^2Cl_2$−*cis*-$RuD^2A^2Cl_2^-$ (lower potential).

a low-energy ligand field band (t_2 splitting) is observed in the expected region (Figure 2, Table 2).

The $RuD_2Cl_2^+$ complexes are stable in dry solvents, and their cyclic voltammograms (initial scan cathodic) are superposable on those of the corresponding RuD_2Cl_2 complexes (initial scan anodic), implying that the redox process is stereoretentive, as implied in eq 2.

Reaction with Water. Rate and Activation Parameters. In wet solutions, $RuD_2Cl_2^+$ reacts spontaneously and quantitatively as in eq 4. The 1:2 ratio of $RuDACl_2$ and RuD_2Cl_2 at

$$3cis/trans\text{-}RuD_2Cl_2^+ + H_2O \rightarrow cis/trans\text{-}RuDACl_2 + 2cis/trans\text{-}RuD_2Cl_2 + 3H^+ \quad (4)$$

completion of the reaction is in accord with the heights of the distinctive voltammetric peaks (couples of eqs 2 and 3) of the two species and spectral intensities (see below) thereof. The voltammetric results for a representative case, viz *cis*-$RuD^2{}_2Cl_2^+$, is depicted in Figure 5. The measurement was carried out by dissolving in acetonitrile the dry residue left after complete removal of solvent and water at the end of the reaction. In essence, the reaction of eq 4 is a disproportionation in which the ligand is oxidized at the expense of the metal which becomes reduced. The amide oxygen originates from water. The transformation proceeds unhindered in oxygen-free environments.

The rate of the reaction of eq 4 is amenable to spectrophotometric examination in 1:6 dichloromethane−acetonitrile solution containing measured amounts of water. The case of *trans*-$RuD^2{}_2Cl_2^+$ is particularly convenient for the study, and details will be presented for this case. The largest changes occur near 700 nm due to the growth of the MLCT band (Table 2) of *trans*-$RuD^2{}_2Cl_2$. The other two species have low absorptions in this region. At the end of the reaction, the absorption at 700 nm corresponds to the conversion of two-thirds of the total ruthenium into *trans*-$RuD^2{}_2Cl_2$ as required by eq 4.

Rates were monitored at 700 nm using the changes in absorption, A_t, as a function of time, *t*. In the presence of excess water (pseudo-first-order conditions) the rate of the transformation is found to be proportional to the concentration of *trans*-$RuD^2{}_2Cl_2^+$, eq 5. Further, the observed rate constant k_{obs} varies

$$\text{rate} = k_{obs}[trans\text{-}RuD^2{}_2Cl_2^+] \quad (5)$$

(12) (a) Pramanik, A.; Bag, N.; Ray, D.; Lahiri, G. K.; Chakravorty, A. *Inorg. Chem.* **1991**, *30*, 410. (b) Pramanik, A.; Bag, N.; Lahiri, G. K.; Chakravorty, A. *J. Chem. Soc., Dalton Trans.* **1992**, 101. (c) Pramanik, A.; Bag, N.; Chakravorty, A. *J. Chem. Soc., Dalton Trans.* **1993**, 237. (d) Pramanik, A.; Bag, N.; Lahiri, G. K.; Chakravorty, A. *J. Chem. Soc., Dalton Trans.* **1990**, 3823.

(13) (a) Bond, A. M.; Colton, R.; Kevekordes, J. E. *Inorg. Chem.* **1986**, *25*, 749. (b) Bond, A. M.; Colton, R.; Kevekordes, J. E.; Panagioditou, P. *Inorg. Chem.* **1987**, *26*, 1430 and reference therein. (c) Bursten, B. E.; Green, M. R. *Prog. Inorg. Chem.* **1988**, *36*, 393 and references therein.

$$k_{obs} = k[H_2O] \quad (6)$$

$$\text{rate} = k[\textit{trans}\text{-}RuD^2{}_2Cl_2{}^+][H_2O] \quad (7)$$

linearly with the concentration of water according to eq 6. Thus the formation of *trans*-$RuD^2A^2Cl_2$ from *trans*-$RuD^2{}_2Cl_2{}^+$ and water follows the second-order rate law of eq 7. Variable-temperature rate constants and the derived activation parameters are listed in Table 6. The large decrease of entropy (~30 eu) in the activation process is suggestive of strong "association" between water and *trans*-$RuD^2{}_2Cl_2{}^+$ in the rate-determining step (rds).

A Reaction Model. The addition of water to the imine function leading to an α-hydroxy amine moiety (>C=N− → >C(OH)NH) is a documented pathway to Schiff base hydrolysis (to >C=O and $-NH_2$).[14] In some instances, the product of addition of water or alcohol has been found to be a stable entity.[15] A plausible rationale for the above-noted close association between the ruthenium(III) α-diimine complex and water is actual addition as expressed by general reaction of eq 8. The crucial requirement is that the adduct **6** (or NH-

$$RuD_2Cl_2{}^+ + H_2O \xrightarrow{rds} \mathbf{6} \quad (8)$$

deprotonated version thereof) must undergo rapid oxidation before the possible hydrolysis-related complications could set in. Two electrons are to be transferred and a plausible route is induced electron transfer:[3,16] **6** → **7** (oxidative radical formation), **7** → **8** (internal redox and proton loss), and **8** → **3** (metal oxidation), eqs 9−11, where $RuD_2Cl_2{}^+$ acts as the external

$$RuD_2Cl_2{}^+ + \mathbf{6} \rightarrow \mathbf{7} + 2H^- + RuD_2Cl_2 \quad (9)$$

$$\mathbf{7} \rightarrow \mathbf{8} + H^+ \quad (10)$$

$$RuD_2Cl_2{}^+ + \mathbf{8} \rightarrow \mathbf{3} + RuD_2Cl_2 \quad (11)$$

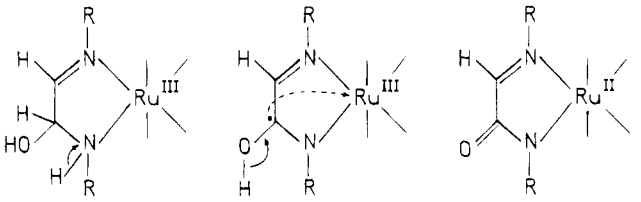

6 **7** **8**

oxidant. The reduction potentials are right for the reaction, and there is no kinetic barrier either. In the prescription of Scheme 1, aqueous cerium(IV) (or hydrogen peroxide) acts as the external oxidant and the whole of RuD_2Cl_2 is thus converted to $RuDACl_2$ via $RuD_2Cl_2{}^+$ according to the stoichiometry stated in eqs 12 and 13.

$$RuD_2Cl_2 + Ce^{4+} \rightarrow RuD_2Cl_2{}^+ + Ce^{3+} \quad (12)$$

$$RuD_2Cl_2{}^+ + H_2O + 2Ce^{4+} \rightarrow RuDACl_2 + 2Ce^{3+} + 3H^+ \quad (13)$$

(14) Keyser, R. H.; Pollack, R. M. *J. Am. Chem. Soc.* **1977**, *99*, 3379.
(15) (a) Harris, C. M.; McKenzie, E. D. *Nature* **1962**, *196*, 670. (b) Busch, D. H.; Bailer, J. C., Jr. *J. Am. Chem. Soc.* **1956**, *78*, 1137. (c) Katovic, V.; Vergez, S. C.; Busch, D. H. *Inorg. Chem.* **1977**, *16*, 1716.
(16) Taube, H. *Electron Transfer Reactions of Complex Ions in Solution*; Academic Press: New York, 1973; p 73.

Table 6. Rate Constants and Activation Parameters for *trans*-$RuD^2{}_2Cl_2{}^+$ in 1:6 Dichloromethane−Acetonitrile[a]

T, K	$[H_2O]$, M	10^3k_{obs}, s^{-1}	10^3k, $M^{-1}\,s^{-1}$	$\Delta H^{\ddagger}$, kcal mol^{-1}	$\Delta S^{\ddagger}$, eu
280	1.11	0.42(0.05)	0.39(0.06)		
	1.67	0.60(0.02)			
	2.22	0.81(0.03)			
	2.78	0.99(0.03)			
288	1.11	0.86(0.06)	0.73(0.05)		
	1.67	1.23(0.02)			
	2.22	1.65(0.01)		12.5(0.9)	−29.9(2.8)
	2.78	2.03(0.06)			
293	1.11	1.23(0.01)	1.16(0.07)		
	1.67	2.05(0.02)			
	2.22	2.54(0.02)			
	2.78	3.20(0.03)			
298	0.56	0.95(0.05)	1.51(0.09)		
	1.11	1.79(0.03)			
	1.67	2.58(0.01)			
	2.78	4.23(0.02)			

[a] Least-squares deviations are given in parentheses.

The oxidation of $Re^{III}(pD)(OPPh_3)Cl_3$, **9**, to $Re^{IV}(pA)(OPPh_3)Cl_3$, **10**, where pD is pyridine-2-carboxaldimine (as in **1**) and pA is the corresponding amide (deprotonated) has been briefly reported from this laboratory.[1] Here the reactive intermediate is $Re^{IV}(pD)(OPPh_3)Cl_3{}^+$, $\mathbf{9}^+$, which disproportionates in water, eq 14, following the rate law of eq 15 ($k = 1.92 \times 10^{-4}\ M^{-1}\ s^{-1}$ at 298 K).[6] In the presence of an external oxidant (Ce^{4+} or H_2O_2), the conversion of **9** to **10** goes to completion.

$$3\,\mathbf{9}^+ + H_2O \rightarrow \mathbf{10} + 2\,\mathbf{9} + 3H^+ \quad (14)$$

$$\text{rate} = k[\mathbf{9}^+][H_2O] \quad (15)$$

Thus the two otherwise very different systems RuD_2Cl_2 and $Re(pD)(OPPh_3)Cl_3$ act as close analogs as far as the aldimine → amide transformation is concerned. At this stage, the following general traits appear to be crucial. (i) The coordinated metal atom should have two easily accessible oxidation states related by facile transfer of one electron (Ru^{2+}, Ru^{3+}; Re^{3+}, Re^{4+}). (ii) The higher oxidation state should have sufficient polarizing effect on the aldimine function to make the carbon site electrophilic enough to promote water binding. (iii) The water adduct should have the ability to undergo rapid electron transfer at ligand and metal sites. These provide a working base for expanding the scope of the aldimine → amide reaction to newer systems.

Concluding Remarks. The main results of this work will now be summarized. The isomeric $Ru^{II}D_2Cl_2$ chelates are shown to be excellent substrates for aldimine → amide transformation, which is found to proceed stereoretentively, affording $Ru^{III}DACl_2$.

The trends of ruthenium(III)−ruthenium(II) reduction potentials (cis > trans) and of transition energies (trans > cis) within the split t_2 shells are consistent with the isomeric geometries of $RuDACl_2$. The same applies to $Ru^{III}D_2Cl_2{}^+$, the product of one-electron oxidation of RuD_2Cl_2 in dry solvents. The metal reduction potentials of $RuDACl_2$ are ~0.5 V lower than those of RuD_2Cl_2. Significantly, the Ru−N(amide) distance is ~0.1 Å shorter than the Ru−N(imine) distance in *cis*-$RuD^2A^2Cl_2$.

The transformation RuD_2Cl_2 → $RuDACl_2$ occurs via $RuD_2Cl_2{}^+$, which reacts with water, affording the amide complex, the entropy of activation being strongly negative. It is proposed that water adds to an imine function and the resultant α-hydroxy amine function is rapidly oxidized to amide by an induced electron transfer route. Our search for newer examples of the

aldimine → amide reaction is continuing with the objective of augmenting and generalizing the ideas presented in this work.

Experimental Section

Materials. Hydrated ruthenium trichloride (Arora Matthey, Calcutta) was purified by repeated treatment with concentrated hydrochloric acid.[17] The complex $Ru(Me_2SO)_4Cl_2$[18] and the glyoxaldiimines[19] were prepared by reported methods. The purification and drying of dichloromethane and acetonitrile for electrochemical and spectral work were done as before.[20] All other chemicals and solvents were of reagent grade and were used without further purification.

Physical Measurements. Electronic spectra were recorded with a Hitachi 330 spectrophotometer fitted with a thermostated cell compartment. Infrared spectra (4000−300 cm^{-1}) were taken on a Perkin-Elmer 783 spectrophotometer, and X-band EPR spectra were recorded on a Varian E-109C spectrometer fitted with a quartz Dewar flask. The spectra were calibrated with respect to DPPH ($g = 2.0037$). Electrochemical measurements (cyclic voltammetry, coulometry, and differential pulse voltammetry) were done by using a PAR Model 370-4 electrochemistry system as described elsewhere.[21] All experiments were performed at a platinum working electrode under dinitrogen atmosphere, the supporting electrolyte being tetraethylammonium perchlorate (TEAP). The potentials are referred to the saturated calomel electrode (SCE) and are uncorrected for junction contribution. Magnetic susceptibilities were measured on a PAR-155 vibrating-sample magnetometer. Solution (10^{-3} M) electrical conductivity was measured by using a Philips PR 9500 bridge. Microanalyses (C,H,N) were done by using a Perkin-Elmer 240C elemental analyzer.

Synthesis of RuD_2Cl_2. *trans*-Dichlorobis(*N,N'*-dicyclohexylglyoxal diimine)ruthenium(II), *trans*-$RuD^1{}_2Cl_2$. The complex $Ru(Me_2SO)_4Cl_2$ (100 mg, 0.20 mmol) was suspended in 20 mL of ethanol, and D^1 (100 mg, 0.45 mmol) was added. The mixture was kept warm at 40 °C for 15 min. The resulting blue solution was evaporated to dryness under reduced pressure. The solid mass thus obtained was dissolved in 5 mL of dichloromethane, and the solution was subjected to chromatography on a silica gel column (20 × 1 cm; 60−120 mesh, BDH). On elution with benzene−acetonitrile (9:1), a deep blue band of the required complex moved rapidly. Upon slow evaporation of the eluent, the complex was obtained as shining blue microcrystals. Yield: 75%. Anal. Calcd for *trans*-$RuD^1{}_2Cl_2$, $RuC_{28}H_{48}N_4Cl_2$: C, 54.90; H, 7.84; N, 9.15. Found: C, 54.65; H, 7.80; N, 9.13.

***cis*-Dichlorobis(*N,N'*-dicyclohexylglyoxal diimine)ruthenium(II), *cis*-$RuD^1{}_2Cl_2$.** The trans isomer (100 mg, 0.16 mmol) was dissolved in 20 mL of ethanol and the solution refluxed for 30 min to give a dark pink solution which afforded the crystalline cis complex in quantitative yield upon solvent evaporation.

The complex was also synthesized by refluxing a 1:2 mixture of $Ru(Me_2SO)_4Cl_2$ and D^1 in ethanol for 30 min. The resulting pink solution was evaporated to dryness under reduced pressure, and the solid mass thus obtained was dissolved in 5 mL of dichloromethane. The solution was subjected to chromatography on a silica gel column (20 × 1 cm; 60−120 mesh, BDH). On elution with benzene−acetonitrile (7:3), a dark pink band moved rapidly and was collected. The required complex was obtained from the eluent as shining dark-colored crystals by slow evaporation. Yield: 85%. Anal. Calcd for *cis*-$RuD^1{}_2Cl_2$, $RuC_{28}H_{48}N_4Cl_2$: C, 54.90; H, 7.84; N, 9.15. Found: C, 54.62; H, 7.78; N, 9.12.

Single crystals of composition *cis*-$RuD^1{}_2Cl_2$·PhMe were obtained by the slow diffusion of toluene into a dichloromethane solution of *cis*-$RuD^1{}_2Cl_2$. Anal. Calcd for *cis*-$RuD^1{}_2Cl_2$·PhMe, $RuC_{35}H_{56}N_4Cl_2$: C, 59.66; H, 7.95; N, 7.95. Found: C, 59.60; H, 7.92; N, 7.91.

***trans*-Dichlorobis(*N,N'*-di-*p*-tolylglyoxal diimine)ruthenium(II), *trans*-$RuD^2{}_2Cl_2$.** The complex $Ru(Me_2SO)_4Cl_2$ (100 mg, 0.20 mmol) was suspended in 20 mL of ethanol, and to the suspension was added D^2 (100 mg, 0.42 mmol). The mixture was refluxed for 30 min and then cooled. A green microcrystalline solid precipitated, which was collected by filtration, washed thoroughly with ethanol, and finally dried in vacuo over P_4O_{10}. Yield: 85%. Anal. Calcd for *trans*-$RuD^2{}_2Cl_2$, $RuC_{32}H_{32}N_4Cl_2$: C, 59.63; H, 4.97; N, 8.69. Found: C, 59.58; H, 4.93; N, 8.62.

***cis*-Dichlorobis(*N,N'*-di-*p*-tolylglyoxal diimine)ruthenium(II), *cis*-$RuD^2{}_2Cl_2$.** This complex was prepared by boiling the trans isomer in diglyme as reported.[4] Anal. Calcd for *cis*-$RuD^2{}_2Cl_2$, $RuC_{32}H_{32}N_4Cl_2$: C, 59.63; H, 4.97; N, 8.69. Found: C, 59.60; H, 4.90; N, 8.60.

Conversion of RuD_2Cl_2 to $RuDACl_2$ by Using Cerium(IV) as Oxidant. One representative case will be described in detail.

***cis*-Dichloro(*N*-cyclohexyl(cyclohexylimino)acetamidato)(*N,N'*-dicyclohexylglyoxal diimine)ruthenium(III), *cis*-$RuD^1A^1Cl_2$.** To a solution of 100 mg (0.16 mmol) of *cis*-$RuD^1{}_2Cl_2$ in 30 mL of dichloromethane−acetonitrile (1:6) was added 230 mg (0.36 mmol) $(NH_4)_4Ce(SO_4)_4·2H_2O$ dissolved in 20 mL of water. The mixture was stirred at room temperature for 15 h. The reaction mixture was then filtered and the filtrate evaporated to dryness under reduced pressure. The reddish brown solid product thus obtained was dried in vacuo over P_4O_{10}. Yield: 88%.

The complexes *trans*-$RuD^1A^1Cl_2$, *cis*-$RuD^2A^2Cl_2$, and *trans*-$RuD^2A^2Cl_2$ were synthesized similarly in 75−85% yields from *trans*-$RuD^1{}_2Cl_2$, *cis*-$RuD^2{}_2Cl_2$, and *trans*-$RuD^2{}_2Cl_2$, respectively. After addition of oxidant, the stirring times in these cases were respectively 10, 2, and 10 h.

Anal. Calcd for *cis*-$RuD^1A^1Cl_2$, $RuC_{28}H_{47}N_4OCl_2$: C, 53.59; H, 7.49; N, 8.93. Found: C, 53.54; H, 7.45; N, 8.90. Found for *trans*-$RuD^1A^1Cl_2$: C, 53.55; H, 7.46; N, 8.91. Anal. Calcd for *cis*-$RuD^2A^2Cl_2$, $RuC_{32}H_{31}N_4OCl_2$: C, 58.27; H, 4.70; N, 8.50. Found: C, 58.22; H, 4.67; N, 8.46. Found for *trans*-$RuD^2A^2Cl_2$: C, 58.20; H, 4.62; N, 8.46.

Single crystals of composition *cis*-$RuD^1A^1Cl_2·CH_2Cl_2$ were grown from the slow diffusion of hexane into a dichloromethane solution of *cis*-$RuD^1A^1Cl_2$. Anal. Calcd for *cis*-$RuD^1A^1Cl_2·CH_2Cl_2$, $RuC_{29}H_{49}N_4OCl_4$: C, 48.89; H, 6.88; N, 7.87. Found: C, 48.85; H, 6.83; N, 7.85.

Conversion of RuD_2Cl_2 to $RuDACl_2$ by Using Hydrogen Peroxide as Oxidant. On representative case will be described.

***trans*-Dichloro(*N*-cyclohexyl(cyclohexylimino)acetamidato)(*N,N'*-dicyclohexylglyoxal diimine)ruthenium(III), *trans*-$RuD^1A^1Cl_2$.** To a solution of 100 mg (0.16 mmol) of *trans*-$RuD^1{}_2Cl_2$ in 30 mL of dichloromethane−acetonitrile (1:6) was added 0.5 mL of 30% H_2O_2, and the mixture was stirred for 10 h. The resulting solution was evaporated to dryness under reduced pressure, and the dark brown solid product was washed thoroughly with water and dried in vacuo over P_4O_{10}. Yield: 78%.

The complex *trans*-$RuD^2A^2Cl_2$ can be similarly prepared from *trans*-$RuD^2{}_2Cl_2$. Hydrogen peroxide can be used for preparing *cis*-$RuDACl_2$ species also, but the yields are poor. Anal. Calcd for *trans*-$RuD^1A^1Cl_2$, $RuC_{28}H_{47}N_4OCl_2$: C, 53.59; H, 7.49; N, 8.93. Found: C, 53.55; H, 7.46; N, 8.91. Calcd for *trans*-$RuD^2A^2Cl_2$, $RuC_{32}H_{31}N_4OCl_2$: C, 58.27; H, 4.70; N, 8.50. Found: C, 58.22; H, 4.57; N, 8.46.

***cis*-Dichlorobis(*N,N'*-dicyclohexylglyoxal diimine)ruthenium(III) Perchlorate, *cis*-$[RuD^1{}_2Cl_2]ClO_4$.** To a solution of 100 mg (0.16 mmol) of *cis*-$RuD^1{}_2Cl_2$ in 30 mL of dichloromethane−acetonitrile (1:6) was added 115 mg (0.18 mmol) of $(NH_4)_4Ce(SO_4)_4·2H_2O$, dissolved in 5 mL of water. The mixture was stirred at room temperature for 5 min. The orange solution was then filtered, and to the filtrate was added a saturated aqueous sodium perchlorate solution (10 mL). An orange solid was obtained upon evaporation of the solvent. It was washed thoroughly with water and dried in vacuo over P_4O_{10}. Yield: 80%. The same product was also obtained by the coulometric oxidation of *cis*-$RuD^1{}_2Cl_2$ in dry 1:6 dichloromethane−acetonitrile (0.1 M in TEAP) at +0.80 V vs SCE. Solvent evaporation and repeated recrystallization from acetonitrile−benzene gave the pure product in

(17) Chakravarty, A. R.; Chakravorty, A. *Inorg. Chem.* **1981**, *20*, 275.
(18) Evans, I. P.; Spencer, A.; Wilkinson, G. *J. Chem. Soc., Dalton Trans.* **1973**, 204.
(19) (a) Kliegman, J. M.; Barnes, R. K. *Tetrahedron* **1970**, *26*, 2555. (b) tom Dieck, H.; Svoboda, M.; Greiser, Th. *Z. Naturforsch., B: Anorg. Chem., Org. Chem.* **1981**, *36B*, 823.
(20) (a) Basu, P.; Pal, S.; Chakravorty, A. *J. Chem. Soc., Chem. Commun.* **1989**, 977. (b) Basu, P.; Bhanja Choudhury, S.; Chakravorty, A. *Inorg. Chem.* **1989**, *28*, 2680. (c) Ray, D.; Chakravorty, A. *Inorg. Chem.* **1988**, *27*, 3292.
(21) Pramanik, A.; Bag, N.; Ray, D.; Lahiri, G. K.; Chakravorty, A. *Inorg. Chem.* **1991**, *30*, 410.

Table 7. Crystallographic Data for *cis*-$RuD^1{}_2Cl_2$·PhMe and *cis*-$RuD^1A^1Cl_2$·CH_2Cl_2

	cis-$RuD^1{}_2Cl_2$·PhMe	*cis*-$RuD^1A^1Cl_2$·CH_2Cl_2
chem formula	$C_{35}H_{56}N_4Cl_2Ru$	$C_{29}H_{49}N_4OCl_4Ru$
fw	704.8	712.6
space group	$P2_1/c$	$P2_1/c$
a, Å	14.808(6)	11.295(4)
b, Å	19.442(7)	27.064(14)
c, Å	13.989(6)	12.064(4)
β, deg	117.18(3)	107.52(2)
V, Å^3	3583(2)	3517(2)
Z	4	4
T, °C	22	22
λ, Å	0.710 73	0.710 73
ϱ_{calc}, g cm^{-3}	1.307	1.346
μ, cm^{-1}	6.15	7.76
transm coeff	0.85−1.00	0.79−1.00
R^a	0.0370	0.0653
$R_w{}^b$	0.0431	0.0695
goodness-of-fit	1.13	1.34

^{a} $R = \sum||F_o| - |F_c||/\sum|F_o|$. ^{b} $R_w = [\sum w(|F_o| - |F_c|)^2/\sum w/F_o|^2]^{1/2}$; $w^{-1} = \sigma^2|F_o| + g|F_o|^2$; $g = 0.0005$ for *cis*-$RuD^1{}_2Cl_2$·PhMe and 0.0001 for *cis*-$RuD^1A^1Cl_2$·CH_2Cl_2. ^{c} The goodness of fit is defined as $[w(|F_o| - |F_c|)^2/(n_o - n_v)]^{1/2}$, where n_o and n_v denote the numbers of data and variables, respectively.

95% yield. Anal. Calcd for *cis*-$[RuD^1{}_2Cl_2]ClO_4$, $RuC_{28}H_{48}N_4O_4Cl_3$: C, 47.29; H, 6.75; N, 7.88. Found: C, 47.26; H, 6.72; N, 7.82.

Kinetic Measurements. The trans isomer of $RuD^2{}_2Cl_2$ was quantitatively oxidized to *trans*-$RuD^2{}_2Cl_2$ via coulometry at +0.60 V versus SCE in a 1:6 mixture of scrupulously dry dichloromethane and acetonitrile (0.1 M in TEAP). Aliquots of this solution were diluted as required, and measured amounts of water were added using a calibrated microsyringe. The presence of acetonitrile in the solvent helped to keep the solution homogeneous after water addition.

The reaction was followed spectrophotometrically at 700 nm. The absorption, A_t, was digitally recorded as a function of time, t, and A_∞ was measured (after 24 h) when the reaction was complete. Values of pseudo-first-order rate constants (k_{obs}) were obtained from the slopes of the highly linear plots of $-\ln(A_\infty - A_t)$ versus t. A minimum of 30 A_t−t data points were used in each calculation. Values of the second-order rate constants (k) were obtained from the slopes of the excellently linear plots of k_{obs} versus [H_2O]. The activation enthalpy and entropy parameters, $\Delta H^\ddagger$ and $\Delta S^\ddagger$, were obtained from variable-temperature (7−25 °C) rates using the Eyring equation. All linear fittings and standard deviation calculations were made by the usual least-squares methods.[22]

X-ray Structure Determination. Dimensions of prismatic crystals were 0.40 × 0.28 × 0.26 mm^3 for *cis*-$RuD^1{}_2Cl_2$·PhMe and 0.36 × 0.27 × 0.12 mm^3 for *cis*-$RuD^1A^1Cl_2$·CH_2Cl_2. Both the crystals were dark-colored, and unless otherwise stated, similar procedures were used for both.

Cell parameters were determined by a least-squares fit of 30 machine-centered reflections ($2\theta = 15-30°$). Data were collected by the ω-scan technique in the range $3° \le 2\theta \le 45°$ on a Siemens R3m/V four-circle diffractometer with graphite-monochromated Mo Kα radiation. Two check reflections monitored after each 98 reflections showed no significant intensity reduction in the case of *cis*-$RuD^1{}_2Cl_2$·PhMe (52 h of exposure), but for *cis*-$RuD^1A^1Cl_2$·CH_2Cl_2, the intensity decreased by 15% during data collection (56 h of exposure). The latter data were corrected for decay (the decay correction range on intensities being 0.8538−1.0000). All data were corrected for Lorentz−polarization and absorption.[23] Of the 5113 ($RuD^1{}_2Cl_2$·PhMe: $h = 0, 16$; $k = 0, 21$; $l = -16, 16$) and 5342 ($RuD^1A^1Cl_2$·CH_2Cl_2: $h = 0, 14$; $k = 0, 33$; $l = -15, 15$) reflections collected, 4707 and 4821 were unique, of which 2986 and 2373 were respectively taken as observed ($I > 3\sigma(I)$) for structure solution and refinement. For both structures, systematic absences corresponded to the space group $P2_1/c$.

The metal atoms were located from Patterson maps, and the rest of the non-hydrogen atoms emerged from successive Fourier syntheses. The structures were then refined by full-matrix least-squares procedures. All non-hydrogen atoms were refined anisotropically, and hydrogen atoms were added at calculated positions with fixed $U = 0.08$ Å^2 in the final cycle of refinement. In *cis*-$RuD^1A^1Cl_2$·CH_2Cl_2, the solvent molecule was disordered. The highest residual were 0.29 and 0.58 e Å^{-3}, respectively, for $RuD^1{}_2Cl_2$·PhMe and $RuD^1A^1Cl_2$·CH_2Cl_2. All calculations were done on a Micro VAX II computer using the SHELXTL-Plus program package.[24] Significant crystal data are listed in Table 7. Selected atomic coordinates and isotropic thermal parameters are collected in Tables 8 and 9.

Table 8. Selected Atomic Coordinates (×10^4) and Equivalent Isotropic Displacement Coefficients^a (Å^2 × 10^3) for *cis*-$RuD^1{}_2Cl_2$·PhMe

	x	y	z	U(eq)
Ru	4283(1)	1514(1)	1245(1)	30(1)
Cl(1)	5526(1)	1547(1)	571(1)	46(1)
Cl(2)	3386(1)	2488(1)	129(1)	48(1)
N(1)	3333(3)	1562(3)	1908(3)	35(2)
N(2)	5029(4)	2181(2)	2504(4)	37(2)
N(3)	4941(3)	635(2)	1996(3)	34(2)
N(4)	3533(3)	800(2)	93(3)	34(2)
C(7)	3610(4)	1961(3)	2743(5)	43(3)
C(8)	4558(4)	2305(3)	3069(5)	43(3)
C(21)	4729(4)	105(3)	1379(5)	41(3)
C(22)	3945(4)	191(3)	314(5)	42(3)

^{a} Equivalent isotropic U defined as one-third of the trace of the orthogonalized $\mathbf{U}_{ij}$ tensor.

Table 9. Selected Atomic Coordinates (×10^4) and Equivalent Isotropic Displacement Coefficients^a (Å^2 × 10^3) for *cis*-$RuD^1A^1Cl_2$·CH_2Cl_2

	x	y	z	U(eq)
Ru	286(1)	1623(1)	1477(1)	39(1)
Cl(1)	−746(4)	2347(1)	563(3)	65(2)
Cl(2)	1820(3)	1656(1)	495(2)	58(1)
O(1)	988(15)	163(4)	1598(9)	132(7)
N(1)	866(10)	968(3)	2171(7)	40(4)
N(2)	−683(10)	1165(4)	120(7)	41(4)
N(3)	−909(10)	1668(3)	2458(8)	47(4)
N(4)	1274(11)	2046(3)	2854(7)	44(4)
C(7)	560(17)	580(5)	1428(11)	66(7)
C(8)	−322(15)	725(5)	285(10)	55(6)
C(21)	−533(16)	1954(5)	3341(10)	55(6)
C(22)	671(17)	2162(5)	3545(12)	60(7)

^{a} Equivalent isotropic U defined as one-third of the trace of the orthogonalized $\mathbf{U}_{ij}$ tensor.

Acknowledgment. Financial support received from the Department of Science and Technology, New Delhi, is gratefully acknowledged. Thanks are expressed to the Council of Scientific and Industrial Research, New Delhi, for providing Fellowship awards to A.P. and M.M.

Supplementary Material Available: For $RuD^1{}_2Cl_2$·PhMe and $RuD^1A^1Cl_2$·CH_2Cl_2, tables of complete bond distances (Tables S1 and S5) and angles (Tables S2 and S6), anisotropic thermal parameters (Tables S3 and S7), hydrogen atom positional parameters (Tables S4 and S8), and atomic coordinates and equivalent isotropic displacement coefficients of non-hydrogen atoms (Tables S9 and S10) (12 pages). Ordering information is given on any current masthead page.

IC941446H

(22) Youden, W. J. *Anal. Chem.* **1947**, *19*, 946.
(23) North, A. C. T.; Philips, D. C.; Mathews, F. S. *Acta Crystallogr.* **1968**, *A24*, 351.
(24) Sheldrick, G. M. *SHELXTL-PLUS 88, Structure Determination Software Programs*; Siemens Analytical X-ray Instruments Inc.: Madison, WI, 1990.